RESEARCH ARTICLE

Resource Allocation in Multi-Cluster Cognitive Radio Networks With Energy Harvesting for Hybrid Multi-Channel Access

AKINBODE A. OLAWOLE AND FAMBIRAI TAKAWIRA, (Member, IEEE)
School of Electrical and Information Engineering, University of the Witwatersrand Johannesburg, Johannesburg 2050, South Africa
Corresponding author: Akinbode A. Olawole (alexolawole@gmail.com)

ABSTRACT Cognitive radio and energy harvesting techniques have been able to provide insight for solutions to the inefficiency in spectrum utilization and the effects of the limited storage capacity of energy batteries. Nevertheless, the requirement for interference constraint for primary user (PU) protection, the quality of service (QoS) requirements of the SUs, and the low power density of the ambient electromagnetic waves have restricted the performance of the radio frequency powered cognitive radio networks (RF-CRNs) in terms of the achievable data rate for specific energy budget or sufficient energy budget for target data rate. We are therefore motivated to investigate a radio frequency powered cognitive radio (RF-CR) with the capacity for improved achievable throughput and energy harvesting. Our model consists of multiple PUs and SUs coexisting in a practical overlapping clustered network. In each time frame for the adopted time division multiple access (TDMA) technique, SUs can exploit the multi-user benefit to harvest energy from both the PU and SUs transmissions for improved active probability. Therefore, taken into consideration the heterogeneity of each SUs in terms of their signal-to-noise (SNR), the energy harvesting rates and the inter- and intra-cluster interference, the problem is formulated into a fractional nonlinear optimization to determine the sensing duration, and power allocations that maximize the average energy efficiency of the RF-CRN subject, to constraints on energy causality, and PU protection. The performance of the proposed hybrid multi-channel access scheme is studied in terms of the trade-off between the total achievable throughput by the secondary users and the interference generated among others. Simulation results show that a trade-off exists between achieving optimal spectral efficiency and energy efficiency and, the optimal transmit power therefore depends on the primary design objective. Results equally show that the proposed hybrid multi-channel access scheme outperforms the existing scheme in literature.

INDEX TERMS Energy efficiency, hybrid multi-channel access, multi-cluster network, radio frequency powered cognitive radio network (RF-CRN), resource allocation (RA).

I. INTRODUCTION

The need for improved spectrum efficiency due to its limited availability and under-utilization, coupled with the recent development in exploiting alternative energy has brought about tremendous research attention towards achieving a wireless and mobile communication networks that are not only spectrum and energy efficient but can equally be pow-

The associate editor coordinating the review of this manuscript and approving it for publication was Rongbo Zhu.

ered more efficiently, conveniently, and with reduced negative impact on the environment. In the radio frequency (RF) energy harvesting-based scheme, spectrum sensing and data transmission activities of the SU among other activities can only occur within the limits of available energy budget. The RF energy arrival is however random, the power density of the ambient RF small hence, the magnitude of the electrical energy that could be derived from the harvested RF energy may not always be sufficient to maximize throughput. This makes the performance of the system (in terms of the sensing

time, the sensing accuracy and the achievable throughput) energy constrained in general. It is therefore imperative that the cognitive radio user (CRU) is energy efficient in terms of balancing the energy consumption with the available harvested energy.

There are three basic cognitive radio access schemes, namely: interweave, underlay and overlay [1]. In the interweave scheme, the secondary user is meant to transmit opportunistically when the PU is determined to be idle on the channel. Underlay system describes a scenario where the secondary user shares the channel with the primary user concurrently but ensure that the interference to the PU is within a tolerable level. Under this system, the SU transmit power is regulated to protect the quality of service (QoS) of the legacy user. In overlay scheme both the SU and PU co-exit on the channel and SU node serves as relay for PU transmission. The cognitive radio transmitters have knowledge of the primary user message, therefore, can improve or maintain the communication of the primary users. Hence, while underlay and overlay techniques permit concurrent cognitive radio and primary users' communication, avoiding simultaneous transmissions with the primary users is the main goal in the interweave access technique. The benefits of both interweave and underlay channel access modes can be jointly utilized by incorporating the underlay channel access mode with the interweave mode in a hybrid interweave/underlay channel access. Therefore, based on the sensing results, the SU can access the channel opportunistically in interweave mode by transmitting his data with high power when the channel is idle. Otherwise, the SU can access the channel in underlay mode with controlled power to avoid causing harmful interference to the PU when the channel is busy.

A. RELATED WORKS

In the specific area of interweave channel access scheme [3], [4], [5], [6], [7], [8], [9], [10], [11], authors in [3], [4] explored the problem of the throughput optimization for the save-then-transmit protocol with variable energy harvesting rate. In particular, while authors in [3], derived the optimal save-ratio as a function of energy harvesting rate, the work in [4], which is inspired by [3] focused on the "harvesting-sensing-throughput" trade-off and joint optimization of the "save-ratio" (i.e. the proportion of the frame length that is required to harvest energy), sensing duration, sensing threshold and the fusion rule to maximize the SU's expected achievable throughput in the EH-CRN. In [5], authors take into consideration the heterogeneity of the SUs in terms of the non-identical harvesting, sensing and reporting characteristics to formulate the problem to determine the active probability, sensing duration, and detection threshold that maximizes the achievable throughput. In [6], the authors employ the finite-horizon partial observable Markov decision process (POMDP) model to derive the optimal policy while satisfying the PU detection and energy causality constraints. [7] investigated a sensing-throughput optimization

problem and focus on the trade-off between sensing time and sum capacity of the SUs with respect to transmission power and sensing time. While the above-mentioned works only considered network scenarios that is either a one-to-one, many-to-one, or one-to-many, the works in [8], [9], [10] explored a multi-channel, multi-user scenario. In [8], the authors investigated a multi-band energy harvesting schemes under cognitive radio interweave framework where, all SUs are allowed to harvest energy from multiple bands of Radio Frequency (RF) sources. The problem was formulated to jointly optimize the number of sensing samples and sensing threshold in order to minimize the sensing time so as to maximize the amount of energy harvested. In [9], authors considered multichannel selection for RF energy harvesting CR networks, where each SU harvests energy from a channel with an active neighboring PU and transmits data on another channel which is not occupied by neighboring PUs. It is required that an SU attempting to transmit data needs to stay in at least one of harvesting zones of active PUs. The problem was formulated to maximize the average throughput of SUs by optimizing the probabilities of accessing channels. In [10], authors considered a cooperative spectrum sensing in a multichannel EH-CRN with two-fold goals which are; to determine the optimal sensing parameter, and to investigate the impact of multiple primary user RF harvesting sources in EH-CRNs. The obtained results showed an improved active probability of cognitive users with increasing number of allocated harvesting sources. Developing an optimal cooperative spectrum sensing strategy in terms of final decision threshold k (in a general $k-out-of-M(k)$ fusion rule), that maximizes the expected achievable throughput of an EH-CRN is a focus of [11].

The underlay channel access scheme is considered in [12], [13], [14], [15], [16]. Pathak and Banerjee in [14] studied energy cooperation among the primary and secondary users to determine the transmit power and energy transfer policy which maximize the total achievable throughput in the underlay scheme. In [16], authors modeled the energy availability at the secondary user (where only one SU is assumed) as first order stationary Markov process and, then proposed an online transmission policy by jointly optimizing the time sharing between harvesting phase and transmission phase, and the transmit time which maximize its average throughput. Multiple SUs were assumed in [12]. Energy harvesting and multiple SUs features were included in [15] with a goal to determine the optimal power control for the harvesting phase and time allocation among the SUs (operating in TDMA) under the constraints of interference and transmit power to maximize the sum throughput of SUs.

Hybrid interweave/underlay access scheme is investigated in [17], [18], [19]. In [17], through monotocity analysis, Zheng et al formulated the problem to determine the optimal detection threshold that maximizes the secondary user throughput. Authors in [18], [19] investigated an hybrid channel access cognitive radio in a network consisting one PU and multiple SUs. More actions are added to the options of

the decision making and energy-based restrictions are applied before taking any action instead of assuming that energy is always sufficient for sensing and transmission. A mixed (full/partial) observable Markov decision process (MOMDP) is introduced to maximize the SU's throughput.

A more robust metric to quantify the performance of cognitive radio network is however, the energy efficiency, which is defined as the ratio of the average achievable throughput to the average energy consumption in the cognitive radio system. Hence, in the context of EH-CRN, energy efficiency can either be considered in terms of throughput maximization for a given energy budget or energy consumption minimization for a target throughput. Enhancing the energy efficiency of the cognitive radio in underlay access mode was studied in [20], [21]. Authors in [20] investigated energy efficient resource allocation and, formulated the problem to jointly determine the channel and the power allocation that maximize the energy efficiency under the transmit power and the interference power constraints. In [21], authors investigated energy efficient maximization of the RF powered CRN under co-interference by jointly optimizing transmission time and transmit power in a network with multiple SUs coexisting with one PU based on underlay channel access scheme.

Energy efficient based hybrid interweave-underlay access mode, is studied in [22], [23], [24]. In [22], authors considered a sensing-based spectrum sharing scheme, and focused their investigation on adapting the transmission power according to the sensing results and determining the optimal power allocation schemes to maximize the energy efficiency of secondary users under constraints on both the transmission and interference power levels. The work in [22] is however based on the conventional energy un-constrained cognitive radios and does not address the constrained energy issues. However, Lee et al in [23] proposed a joint sensing time and power allocation scheme that maximize the energy efficiency of SU in EH-CRN. A single SU, single PU modeled was assumed and it is expected that the SU can only harvest RF energy from the PU transmission during spectrum sensing. With a goal to maximize the outage energy efficiency (OEE) for the un-manned aerial vehicle-assisted energy harvesting cognitive radio network (UAV-EH-CRN), subject to constraints of energy, transmission power, and interference power, [24] considered a hybrid interweave-underlay channel access scheme where, based on the sensing results of the primary user (PU), the UAV can adaptively adjust power to transmit with the destination receiver. The works presented in [23], [24] however, assumed only one PU and one SU network scenario.

Clearly, the focus of the aforementioned works is either on underlay, interweave, or hybrid access mode to either maximize achievable throughput or energy efficiency on one PU channel. It has equally been assumed that SUs can harvest RF from only the PU signal in order to carry out its sensing and data transmission duties. Studies on energy efficiency for hybrid interweave/underlay access scheme in a practical multi-channel, multi-user cognitive radio networks

environment are however, yet to receive considerable attention to the best of our knowledge. The above literature review is summarized in Table 1 where a research gap can be identified.

In this paper, energy efficient resource allocation in a hybrid interweave/underlay access based CRN with energy harvesting capabilities is investigated. The work considers a multi-user, multi-channel, overlapping clustered network with cooperative spectrum sensing. Moreover, by taking the advantage of the multi-user scenario, the amount of harvested energy can be increased for improved active probability of the SUs to sense and to transmit. Different from the existing work in the literature, our model consists of multiple PUs and SUs co-existing in a practical overlapping clustered network and, in each time frame, SUs can harvest RF from both the PU and SUs signal. Therefore, taking into consideration the heterogeneity of the SUs in terms of their SNR, the harvested energy, the intra- and inter-cluster interference, the problem is formulated to determine the optimal power allocations, and the sensing duration, that maximize the average energy efficiency of the cognitive radio users, subject to the constraints on energy causality, PU protection, and interference level on the legacy users. Different from the existing works in the literature, this work focuses on hybrid (interweave/underlay) multi-channel access scheme in a clustered RF-CRN with considerations for the effects of intra- and inter-cluster interference on the PUs and SUs transmissions, and the heterogeneity of the SUs in terms of the harvested energy and their signal-to-noise ratio. The resulting nonlinear, non-convex formulated problem is solved iteratively using an alternating convex optimization method. The summary of main contributions are as follows

B. MAIN CONTRIBUTIONS

1) The RF-CRN is considered for hybrid interweave/ underlay access scheme in a multi-user, multi-channel environment with cooperative spectrum sensing. The paper models a many-to-many overlapping clustered network where an SU is assumed to be assigned to multiple PU channels and multiple SUs assigned to a PU channel. This is different from the existing work in RF-CRN for the hybrid interweave/underlay access scheme (e.g. [23], [24]), as they have mainly focused on one-to-one or one-to-many network models only.

2) Introduces the concept of two frequencies for the hybrid underlay/interweave access schemes. In particular, each cognitive radio user is pre-assigned a pair of frequencies (channels), designated as; the principal transmit channel (PTC) f_j where, SUs can opportunistically transmit on interweave mode and harvest RF energy, and the backup transmit channel (BTC) $f_{j'}$ where SU can only transmit underlay with regulated amount of power (to satisfy the interference constraint and energy causality constraint). To the best of our knowledge, this is the first work that has

TABLE 1. Literature review summary.

Paper no	Interweave	Underlay	Hybrid	Energy Harvesting	Multiple SUs	Multiple PUs	Objective Function	Overlapping Cluster Network	Multiple Frequency Access / SU
[3], [4]	✓			✓			Throughput		
[5], [7], [11]	✓			✓	✓		Throughput		
[8], [9], [10]	✓			✓	✓	✓	Throughput		
[13]		✓					Throughput		
[14], [16]		✓			✓		Throughput		
[12]		✓				✓	Throughput		
[15]		✓			✓	✓	Throughput		
[6]		✓		✓	✓	✓	Throughput		
[17]			✓	✓			Throughput		
[18], [19]			✓	✓	✓		Throughput		
[20], [21]		✓		✓	✓		Energy Efficiency		
[22]			✓				Energy Efficiency		
[23], [24]			✓	✓			Energy Efficiency		
This paper			✓	✓	✓	✓	Energy Efficiency	✓	✓

considered hybrid interweave/underlay multi-channel access scheme in CRN.

3) The performance of the hybrid multi-channel access scheme in the RF-CRN is evaluated in terms of the transmit power allocations, energy efficiency, the data transmission rate, spectrum sensing duration, and the effects of the inter-cluster and intra-cluster interference on the QoS of the network. Simulation results show that there can be improved energy harvesting in the TDMA based RF-CRN for enhanced active probability and hence, improved achievable throughput of SUs if the multi-user scenario can be exploited. Nevertheless, a trade-off exists between harvested energy and the achievable throughput of each SU, thus an optimum number of SU exists where the average throughput of each SU is maximized. Results equally show that the proposed two-frequencies model for the RF-CRN multi-channel access scheme outperforms the existing one-frequency based access in literature in terms of spectral and energy efficiency.

The rest of this paper is organized as follows. Section II discusses the system models, assumptions, and the problem formulation. The solution to the problem is presented in Section III while, the performance evaluation of the proposed scheme is presented in Section IV. This is followed by the conclusion in Section V

II. SYSTEM MODEL AND PROBLEM FORMULATION

This section describes the model, assumptions and problem formulations for the resource allocation and management in the multi-channel access based RF-CRNs.

A. COGNITIVE RADIO NETWORK MODEL

The paper considers a scenario where N secondary users and M primary users co-exist on a network. We assume two levels (classes) of clustering namely, the users' association which is a result of a many-to-many assignment targeted to minimizing the probability of miss-detection of PUs as

TABLE 2. List of notations.

Symbol	Description
N	Number of SUs in the network
M	Number of PUs and PU channels in the network
y_i^j	Received signal at SU i terminal from PU j
d_i^j	Distance between PU j and SU i
$d_{i,k}$	Distance between SU i and SU k, where $i \neq k$
SU_i^j	SU i in cluster j
$SU_{i'}^{j'}$	SU i' in cluster j'
$e_{c,i}^j$	Energy consumed by SU i in cluster j
$P_{u,i}^{j'}$	Underlay power for SU i in cluster j'
$P_{o,i}^j$	Interweave power for SU i in cluster j
$P_{u,i'}^j$	Underlay power for SU i' in cluster j
$P_{o,i'}^{j'}$	Interweave power for SU i' in cluster j'
h_r^j	Channel gain between PU in cluster j and receiver SU r
$h_{i,r}$	Channel gain between i^{th} SU and receiver SU r
h_i^j	Channel gain between the PU and the ith SU in cluster j
$h_{i'}^{j'}$	Channel gain between the PU and the i'^{th} SU in cluster j'
h_i^{jr}	Channel gain between the PU receiver and the ith SU transmitter in cluster j
$h_{i,k}$	Channel gain between SUs i and k ($i \neq k$) in cluster j
$h_{i',r}$	Channel gain between SUs i' and r in clusters j' and j respectively
$h_{i'}^j$	Channel gain between SUs i' and PU in cluster j
$h_i^{j'}$	Channel gain between SUs i and PU in cluster j'
γ_i^j	Signal-to-noise ratio of PU in j as measured by SU i
$\bar{\gamma}$	Average signal-to-noise ratio
$P_{D,i}^j$	Probability of detection of SU i on channel j
$P_{M,i}^j$	Probability of miss-detection of SU i on channel j
$P_{E,i,c}$	Probability of reporting error from SU i to cluster head c
Q_M^j	Cooperative probability of miss-detection for channel j
Q_F^j	Cooperative probability of false alarm for channel j
x_i^j	Assignment variable
χ	Assignment Matrix
K	Number of channel sensed by each user
n_t	Number of SUs allocated to transmit on a channel
N_0	Noise power
σ_{PU}	Interference from transmitting PU
$\sigma_{in}^{j'}$	Total interference from other SUs in cluster j' transmitting on channel f_j

was considered in [10] and, then the channel access (transmission) clusters which is disjointed and in which, jth PU
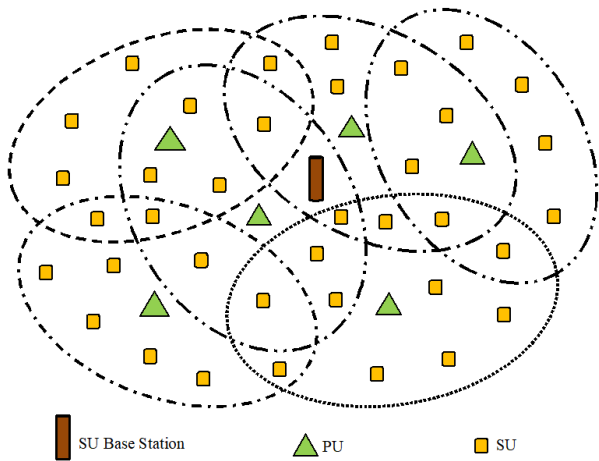
FIGURE 1. Multi-user, multi-channel many-to-many overlapping cluster network model.

FIGURE 2. System model illustrating the frame structure of the cooperative spectrum sensing activities in RF-CRNs. The transmission period is divided into n_t slots ($S1, S2, \cdots Sn_t$), where n_t is the number of SUs allocated to each channel for opportunistic access.

($j = \{1, \ldots, M\}$) only associated with $nt = \{1, \ldots, n_t\}$, ($n_t \in N$) SUs having the least probability of miss-detection or highest gain on the jth channel. In the latter, the cluster with jth PU is designated as cluster j. While the channel assignment clusters are overlapping as shown in Figure 1, the transmission clusters are disjointed. We do not consider clustering or channel assignment in this manuscript. Therefore, we pre-assigned SU i (which belongs to cluster j) to transmit interweave on channel j but transmit underlay on channel j', where cluster j and j' are non-overlapping. For every SU i channel j is designated the PTC and channel j' designated as the BTC. The many-to-many assignment is to ensure shared participation of SUs in cooperative spectrum sensing for improved sensing quality therefore, we referred to the overlapping clusters as sensing clusters. It is expected that each SU cooperatively sense the multiple channels. The secondary users' network includes a secondary user base station otherwise refers to as central controller (CC) located within the transmission range of the SUs. The CC gathers the individual SU parameters such as the evaluated non-cooperative probability of miss-detection, the channel list, and the co-ordinates of the SUs locations. The CC is responsible for the frequency assignment based on the received information from the SUs.

The network is considered to operate on a time slotted basis. The operations of the active energy harvesting secondary users (EH-SUs) is illustrated in Fig. 2. The cluster formation (or channel assignment) which precedes the sensing-transmission/ harvesting frame is assumed. As shown in Fig. 2, the frame length T is divided into sensing phase with duration τ_s, the cooperative sensing overhead τ_r, and the transmission phase of period $\tau_T = T - \tau_s - \tau_r$. Steady state is assumed within each frame, that is, the channel status does not change within a frame. Data transmission is based on TDMA scheme, and the number of transmission slots in the data transmission phase $\tau_T = \tau_s - \tau_r$ is assumed equal to the number of secondary users assigned to transmit in the respective cluster.
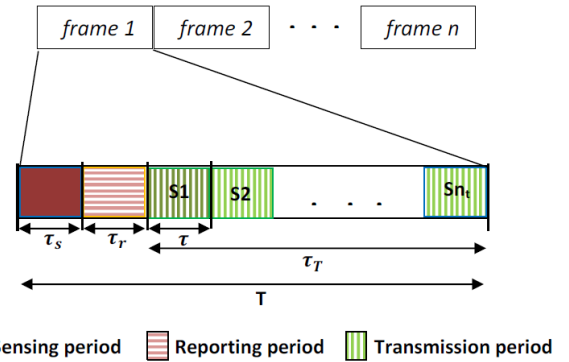
The sensing-transmitting-harvesting model can be described in the following steps:

1) Spectrum sensing phase: Before spectrum sensing, it is assumed that the battery contains an initial energy $e_{i,n}$ which is greater or equal to the amount of energy required for cooperative sensing. During the sensing phase $[0, T_s]$ where, $T_s = \tau_s + \tau_r$, the energy consumed by spectrum sensing and overhead is given as $E_s = p_s \tau_s + e_r$.

2) Data transmission phase: During time interval $[T_s, T]$, if the presence of PU is not detected on the PTC f_j, the SU transmits its data on interweave mode on the channel for a duration corresponding to $\frac{1}{n_t}(T - \tau_s - \tau_r)$ and harvest from other SUs transmitting interweave (from cluster j) and those transmitting underlay (from cluster j') on frequency f_j for the remaining period, i.e. $\left(1 - \frac{1}{n_t}\right)(T - \tau_s - \tau_r)$. Otherwise, the SU transmits underlay on frequency $f_{j'}$ for a period $\frac{1}{n_t}(T - \tau_s - \tau_r)$ using a regulated power and, harvest from the PU signal and, from other SUs in the cluster j' transmitting underlay on f_j for the remaining period i.e. $\left(1 - \frac{1}{n_t}\right)(T - \tau_s - \tau_r)$.

B. PRIMARY NETWORK MODEL
A primary network (PN) with M narrowband spectrum (channels) is considered. The network equally comprises of M PUs that share these spectrum, such that each PU is licensed to one channel. The primary user traffic on each channel is modeled as a time homogeneous discrete Markov process as assumed for example in [5]. Therefore, the spectrum randomly alternates its states between the channel being vacant and occupied. If S_n^j denotes the spectrum occupancy state of channel j on frame n, then the binary hypothesis of the channel status can be represented as $S_n^j \in \{0(vacant), 1(busy)\}$. The steady state probabilities of the channel being idle and busy are denoted as $P(H_0)$ and $P(H_1)$.

C. COOPERATIVE SPECTRUM SENSING

Spectrum sensing is executed during the sensing phase. Assuming a complex value PSK modulated signal and circularly symmetric complex Gaussian (CSCG) noise for primary signal and additive noise in the wireless channel, the probabilities of detection and false alarm as evaluated by SU i on channel j can be expressed as

$$P_{D,i}^j = Q\left(\left(\frac{\varepsilon_i^j}{\sigma_w^2} - \bar{\gamma}_i^j - 1\right)\sqrt{\frac{\tau_c f_s}{2\bar{\gamma}_i^j + 1}}\right) \quad (1)$$

$$P_{F,i}^j = Q\left(\left(\frac{\varepsilon_i^j}{\sigma_w^2} - 1\right)\sqrt{\tau_c f_s}\right) \quad (2)$$

where, ε_i^j, $\bar{\gamma}_i^j$, f_s and σ_w denote the detection threshold of SU i on channel j, the average signal-to-noise ratio (SNR) of channel j at SU i, the sampling frequency and the noise variance respectively. The probability of a miss-detection can be obtained from (1) as

$$P_{M,i}^j = 1 - P_{D,i}^j \quad (3)$$

The cooperative probability of detection and the cooperative probability of false alarm for each channel based on OR decision fusion are evaluated as

$$Q_D^j = 1 - \prod_{i=1}^{N}\left(1 - P_{D,i}^j\right)^{x_i^j}, \quad (4)$$

$$Q_F^j = 1 - \prod_{i=1}^{N}\left(1 - P_{f,i}^j\right)^{x_i^j}, \quad (5)$$

The parameter $x_i^j \in \{0, 1\}$ denotes the assignment decision where, the assignment matrix $\chi = \{x_i^j\}_{M \times N}$ [10] is assumed. The OR rule is adopted as a decision fusion rule being the best rule in protecting the PU signal from interference from the SUs in a Rayleigh fading, and equally the optimal rule in minimizing the total error for a large detection threshold regime.

D. TRANSMISSION MODEL

For transmission purposes, an SU can transmit on only one channel during a transmission frame. Therefore, an SU belongs to a particular cluster j with frequency f_j referred to as PTC from which it can transmit on interweave mode, but also pre-assigned to another frequency $f_{j'}$ referred to as BTC in another cluster j' from which it can transmit underlay. The choice of the two frequencies (for each SU) could be based on the received signal-to-noise ratio (SNR) of the respective PU signals on those channels. Each SU is therefore, pre-assigned to a pair of frequencies $(f_j, f_{j'})$ as interweave frequency, and underlay frequency. Therefore, this paper presents a network scenario (different from what exist in the literature to the best of our knowledge) where the effect of inter-cluster interference on the achievable capacity and performance of the cognitive radio users is taken into consideration.
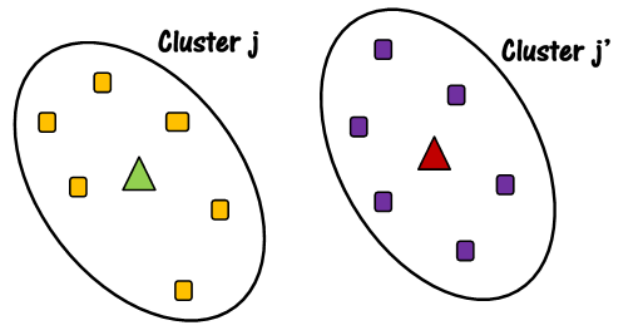

FIGURE 3. Simplified network model showing two-independent clusters / frequencies for each secondary user.

For the purpose of analysis, the network is equivalent to multiples of two-independent clusters referred to as transmission clusters. Figure 3 shows a pair of such independent clusters (j, j') for SU i. The interweave frequency f_j is selected as the frequency with the highest SNR (or best channel gain) at SU i. SUs in this cluster are very close to the PU on channel j. They can sense the channel with high sensing accuracy for high throughput of the secondary users and quality of service (QoS) of the primary users. The underlay frequency $f_{j'}$ in cluster j' is selected among the channels with low SNR at SU i. SU i in cluster f_j could be far from the users in cluster j' so that SUs in j can transmit underlay on $f_{j'}$ with minima interference to the PU and SU signals in cluster j'. Hence, we distinguished between sensing clusters (i.e., overlapping) and transmission clusters (i.e., disjointed). Each SU transmits interweave on f_j or underlay on $f_{j'}$ depending on the spectrum sensing outcome of f_j. In the interweave mode, the SU opportunistically accesses the PTC f_j whenever it is determined vacant. In underlay mode, SU co-exits with a PU on the BTC, $f_{j'}$ but ensures that the interference from the SU remains below a certain threshold. The distance between PUj and SUi is denoted as d_i^j whereas the distance between SUi and SUk ($i \neq k$) is represented as $d_{i,k}$. Both d_i^j and $d_{i,k}$ are random values, since the deployment of SUs are random.

It is assumed that the secondary user network is scheduled to transmit on time division multiple access (TDMA) protocol in both interweave and underlay mode. Therefore, the transmission period in each frame is further divided into (data transmission) slots, and each SU is allocated a slot on the PTC and BTC.

E. ENERGY MODEL

It is assumed that the SU can only perform either spectrum sensing followed by data transmission or energy harvesting at a time. Therefore, the charging process must stop while the SU draws energy to either sense the spectrum or transmit the data in its queue. The power consumption by each SU for spectrum sensing, cooperative sensing overhead, and data transmission activities are denoted as p_s, p_r, and p_t respectively. The total energy consumption by SU i in the nth frame

denoted as $e_{c,i,n}$ can be expressed as $e_{c,i,n} = e_s + e_r + \frac{\tau_T}{n_t} p_{t,i}$ where, $\tau_T = T - \tau_s - \tau_r$ is the data transmission time and n_t denotes the number of SUs assigned to transmit on a channel. It is assumed that the SU must have enough residue energy at the beginning of each frame to participate in spectrum sensing. The (residue) energy state of the SU at the beginning of the nth frame is denoted as $e_{i,n}$. Hence, the minimum energy required for each SU to be active in the network is $e_{i,n} = (p_s \tau_s + p_r \tau_r)$.

The secondary users harvest RF energy from both the transmitting primary user and other secondary users transmitting on the PTC channel. The total average harvested energy is typically modeled as

$$E_{h,i} = \eta_\rho \tau_T \left(h_i^j \varphi_p p_p^j + \sum_{i,k \in n_t} h_{i,k} \varphi_o p_{o,k} + \sum_{i,i' \in n_t} h_{i,i'} \varphi_u p_{u,i'} \right) \quad (6)$$

where, $\rho = ((n_t - 1)/n_t)$ and, h_i^j, $h_{i,k}$, $h_{i,i'}$ denote the channel gain between the PU transmitter and the SUs in cluster j, the channel gain between the SUs i and SU k ($i, k \in n_t$) in cluster j and, channel gains between SUs in cluster j and SUs in cluster j', φ_p, φ_o, φ_u denote the probability the channel j is busy with PU signal, the probability that the channel is busy with SUs in cluster j transmitting interweave and, the probability that the channel is busy with SUs in cluster j' transmitting underlay on channel j. The parameter $0 \leq \eta_{\leq 1}$ denotes the fixed energy conversion efficiency of SU. Linear energy harvesting model is assumed similar to other work in literature [5]. There are different energy harvesting models, e.g., linear EH model [5], [23] and, non-linear EH [25]. However, the investigation of the impact of the EH model on the system performance is out of the work scope. Moreover, our objective is to introduce the concept of two frequencies among others into the hybrid access scheme and, it is our belief that the outcome of our investigation cannot be affected significantly by the way the energy harvesting is modeled.

When the harvested and consumed energy are both put into perspective, the energy in state S_a, $a \in \{1 \cdots 4\}$ at the beginning of the next $(n + 1)^{th}$ frame for an infinite energy storage capacity device can be updated as

$$e_{i,n+1}^{S_a} = max\{0, [e_{i,n} + e_{h,i,n}^{S_a} - e_{c,i,n}^{S_a}]\} \quad (7)$$

where, $e_{h,i,n}^{S_a}$ and $e_{c,i,n}^{S_a}$ denote the harvested RF energy and the energy consumed at state S_a respectively.

F. PROBLEM FORMULATION

In this section, a multi-channel access based RF powered cognitive radio network is considered. In particular, we investigate a scenario where SUs can opportunistically transmit hybrid interweave/underlay scheme on two different frequencies and, harvest RF from both PU and transmitting SUs. The idea of harvesting from other transmitting SUs is particularly

useful in a network where some primary user (RF source) services may be inactive for a substantial period of time (e.g., digital TV broadcasting), and the stored energy in the SUs could get depleted resulting in outages. The summary of the possible states S_i, $i \in \{1, \cdots, 4\}$ of the scheme during the nth frame are as follows:

1) *State 1* (S_1): The PTC is correctly detected to be idle with probability $P_{00} = P_{H_0}(1 - Q_F^j)$. SUs transmit using interweave mode on the PTC frequency, f_j. SUs in cluster j can not harvest from the PU but can harvest from the neighbour SUs in cluster j transmitting on interweave mode with $p_{o,i}$ and from the SUs in j' transmitting underlay on frequency f_j. However, RF energy harvested in the nth frame can only be used in the $(n + 1)^{th}$ frame. The energy consumed and the average harvested energy in this state can be expressed respectively as

$$e_{c,i}^{S_1} = p_{o,i}^j \frac{\tau_T}{n_t} + e_s + e_r \quad (8)$$

and

$$e_{h,i}^{S_1} = \frac{\tau_T}{n_t} \sum_{\substack{i=1,k=1 \\ k \neq i}}^{n_t} p_{o,k}^j h_{k,i} + \frac{\tau_T}{n_t} \sum_{i'=1}^{n_t} p_{u,i'}^j h_{i',i} \left(P_{H_1}' Q_D^{j'} + P_{H_0}' Q_F^{j'} \right) \quad (9)$$

where, $p_{u,i'}^j$, P_{H_1}', P_{H_0}', $Q_D^{j'}$ and $Q_F^{j'}$ represent the underlay transmit power of the SUs in cluster j' transmitting on frequency f_j and the sensing parameters of the SUs in cluster j' respectively.

2) *State 2* (S_2): The PTC incorrectly detected to be vacant (miss-detection) with probability $P_{01} = P_{H_1}(1 - Q_D^j)$. In this state, the SU would transmit using interweave scheme with power $p_{o,i}$ on the PTC f_j during the transmission phase. The transmission would however interfere with the primary user's signal, and little or nothing is gained in terms of throughput. Since harvesting does not depend on the SUs sensing decision, the SU would be able to harvest from both the PU and the SUs transmitting on f_j. The energy consumed and the average harvested energy in this state can be expressed respectively as

$$e_{c,i}^{S_2} = p_{o,i}^j \frac{\tau_T}{n_t} + e_s + e_r \quad (10)$$

and

$$e_{h,i}^{S_2} = p_p^j \rho \tau_T h_i^j + \frac{\tau_T}{n_t} \sum_{\substack{i=1,k=1 \\ k \neq i}}^{n_t} p_{o,k}^j h_{k,i} + \frac{\tau_T}{n_t} \sum_{i'=1}^{n_t} p_{u,i'}^j h_{i',i} \left(P_{H_1}' Q_D^{j'} + P_{H_0}' Q_F^{j'} \right) \quad (11)$$

The second expression on the right hand side (RHS) of (11) represents the sum of the energy harvested from the SUs transmitting on interweave mode ($p_{o,i}$) on f_j.

3) *State 3 (S_3):* The PTC is incorrectly detected to be busy (false alarm) with probability $P_{10} = P_{H_0}Q_F^j$. Each SU transmits using underlay scheme with a regulated amount of power $p_{u,i}$ on frequency $f_{j'}$ for a period $\frac{1}{n_t}\tau_T$ during the transmission phase. SUs can only harvest from the SUs in j' cluster transmitting with underlay power $p_{u,i'}$ on channel f_j

$$e_{c,i}^{S_3} = p_{u,i}\frac{\tau_T}{n_t} + e_s + e_r \qquad (12)$$

and

$$e_{h,i}^{S_3} = \frac{\tau_T}{n_t}\sum_{i'=1}^{n_t} p_{u,i'}^j h_{i',i}\left(P'_{H_1}Q_D^{j'} + P'_{H_0}Q_F^{j'}\right) \qquad (13)$$

4) *State 4 (S_4):* The PTC is correctly detected to be busy with probability $P_{11} = P_{H_1}Q_D^j$. In this state, each secondary user in cluster j transmits underlay on the BTC with a regulated amount of power $p_{u,i}$ for a period $\frac{1}{n_t}\tau_T$ during a transmission phase. The secondary user harvest RF energy from the PU signal on f_j for a period of $\hat{\tau}_h$ (where, $\hat{\tau}_h = \tau_T\left(1 - \frac{1}{n_t}\right) = \tau_T\rho$ represents the period of harvesting during the transmission phase when the SU is not transmitting). The energy consumed and the average harvested energy in this state can be expressed respectively as

$$e_{c,i}^{S_4} = p_{u,i}\frac{\tau_T}{n_t} + e_s + e_r \qquad (14)$$

and

$$e_{h,i}^{S_4} = p_p^j \rho \tau_T h_i^j$$
$$+ \frac{\tau_T}{n_t}\sum_{i'=1}^{n_t} p_{u,i'}^j h_{i,i'}\left(P'_{H_1}Q_D^{j'} + P'_{H_0}Q_F^{j'}\right) \qquad (15)$$

where, $P'_{H_0}Q_F^{j'}$ and $P'_{H_1}Q_D^{j'}$ are the probabilities that the BTC status is a false alarm and 'busy' respectively. The parameter h_i^j denotes the channel gain between SU i and PU j in cluster j. Generally, it is assumed that $P'_{H_1} = P_{H_1}$, and $P'_{H_0} = P_{H_0}$. The second expression on the right hand side (RHS) of (15) represents the average sum of the energy harvested from the SUs in BTC transmitting underlay on frequency f_j.

The different states ($S_1, \cdots, S_4$) represent the status of the PTC. Therefore, the analysis above shows that the SU can opportunistically harvest energy in every frame. The average energy harvested by SU i can be expressed as

$$E_{h,i} = \sum_{a=1}^{4} \eta e_{h,i}^{S_a}$$
$$= \eta_\rho \tau_T \left\{ \sum_{\substack{i=1 \\ k=1 \\ i\neq k}}^{n_t} p_{o,k}^j h_{i,k}\left(P_{H_0}(1 - Q_F^j) + P_{H_1}(1 - Q_D^j)\right)\right.$$
$$\left. + p_p^j h_i^j P_{H_1}Q_D^j + \sum_{i'=1}^{n_t} p_{u,i'}^j h_{i,i'}\left(P'_{H_1}Q_D^{j'} + P'_{H_0}Q_F^{j'}\right)\right\} \qquad (16)$$

where, the first and second expressions on the RHS of the (16) represents the average harvested energy from the SUs in cluster j transmitting interweave on frequency f_j and, the average energy harvested from the PU on frequency f_j during SU transmission phase respectively. The third expression denotes the average harvested energy from the SU in cluster j' transmitting underlay on f_j. The parameters $P'_{H_0}Q_F^{j'}$ and $P'_{H_1}Q_D^{j'}$ express the probability of the status of the PU in cluster j' while, η_h denotes the energy harvesting efficiency. SUs in cluster j' can only transmit underlay on frequency f_j when $f_{j'}$ is busy or presumed to be busy (false alarm). The parameters Q_D^j and Q_F^j denote the cooperative probabilities of detection and that of false alarm of the PTC f_j respectively, whereas, $Q_D^{j'}$ and $Q_F^{j'}$ denote the cooperative probabilities of detection and that of false alarm of the BTC $f_{j'}$.

The average energy consumed by SU i denoted as $e_{c,i}$ can explicitly be expressed as

$$E_{c,ave} = \sum_{a=1}^{4}\sum_{i=1}^{n_t} e_{c,i,}^{S_a}$$
$$= e_s + e_r + \frac{\tau_T}{n_t T}\left\{\left[P_{H_0}Q_F^j + P_{H_1}Q_D^j\right]p_{u,i}^{j'}\right.$$
$$\left. + \left[P_{H_0}(1 - Q_F^j) + P_{H_1}(1 - Q_D^j)\right]p_{o,i}^j\right\}. \qquad (17)$$

The average throughput of SU, taken into consideration both the intra-cluster and inter-cluster interference of users among the two clusters can be expressed as in (18)

$$R(\tau_s, \varepsilon_i^j, p_{o,i}, p_{u,i})\big|_{\sigma_{un}^{j'}\neq 0, \sigma_{ov}^{j'}\neq 0}$$
$$= \frac{\tau_T}{n_t T}\left[P_{H_0}\left(1 - Q_{F,j}\right)\sum_{i=1}^{n_t}\log_2\left(1 + \frac{h_{i,r}p_{o,i}^j}{N_0 + \sigma_{i',(un)}^{j'}}\right)\right.$$
$$+ P_{H_1}\left(1 - Q_{D,j}\right)\sum_{i=1}^{n_t}\log_2\left(1 + \frac{h_{i,r}p_{o,i}^j}{N_0 + \sigma_{PU}^j + \sigma_{i',(un)}^{j'}}\right)$$
$$+ P_{H_0}Q_{F,j}\sum_{i=1}^{n_t}\log_2\left(1 + \frac{h_{i,r}p_{u,i}^{j'}}{N_0 + \sigma_{PU}^{j'} + \sigma_{i',(ov)}^{j'}}\right)$$
$$\left. + P_{H_1}Q_{D,j}\sum_{i=1}^{n_t}\log_2\left(1 + \frac{h_{i,r}p_{u,i}^{j'}}{N_0 + \sigma_{PU}^{j'} + \sigma_{i',(ov)}^{j'}}\right)\right] \qquad (18)$$

where, $\tau_T = T - \tau_s - \tau_r$ and N_0 denote the transmission slot and the noise variance. The parameters

$$\sigma_{i',(un)}^j = \left(P'_{H_1} Q_D^{j'} + P'_{H_0} Q_F^{j'} \right) p_{u,i'}^j h_{i',r}$$
$$\sigma_{i',(ov)}^{j'} = \left(P'_{H_1}(1 - Q_D^{j'}) + P'_{H_0}(1 - Q_F^{j'}) \right) p_{o,i'}^{j'} h_{i',r}$$
$$\sigma_{PU}^{j'} = p_p^{j'} h_r^{j'}$$
$$\sigma_{PU}^j = p_p^j h_r^j \qquad (19)$$

denote the average interference from SU i' in cluster j' transmitting underlay on f_j, the average interference of SU i' in cluster j' transmitting interweave on $f_{j'}$ but interfering with the SU signal in j transmitting underlay on $f_{j'}$, interference from PU in $f_{j'}$, and interference from PU in f_j respectively. Different from e.g., [17], [18], [19], [22], [23], [24], Equation (18) models the total achievable average throughput of the SUs transmission in a practical wireless channel environment by taking into consideration the effect of both intra-cluster and inter-cluster interference on the achievable throughput of the secondary user transmission.

The average transmit power constraint at the SU transmitter during the data transmission phase should be considered as:

$$p_{av,i} = \left\{ \left[P_{H_0}(1 - Q_F^j) + P_{H_1}(1 - Q_D^j) \right] p_{o,i}^j \right.$$
$$\left. + \left[P_{H_0} Q_F^j + P_{H_1} Q_D^j \right] p_{u,i}^{j'} \right\} \leq p_{max}. \qquad (20)$$

where p_{max} is the allowed maximum average transmit power. Moreover, while considering the hybrid multi-channel access, it is essential that the interference caused by the secondary users to the primary user must be regulated in order to guarantee the quality of service (QoS) of the PUs. Therefore, the average interference from the SUs in cluster j to the primary users in j and j' that is, I_s^j should satisfy the following conditions

$$I_s^j = h_i^{j,r} p_{o,i}^j P_{H_1}(1 - Q_D^j)$$
$$+ \left\{ h_i^{j'r} p_{u,i}^{j'} \left[P'_{H_1}(1 - Q_D^{j'}) + P_{H_0} Q_D^{j'} \right] \right\} \leq I_{max}$$
$$\forall \, i \in \{1, \ldots n_t\}, \qquad (21)$$

where, I_{max} is the maximum tolerable interference to the primary user. The first expression on the LHS of inequality in (21) denotes the interference from SU i in cluster j transmitting interweave on PTC f_j and the second expression represents the interference from SU i in cluster j transmitting underlay on BTC $f_{j'}$.

The objective of is to jointly determine the sensing duration (τ_s), the power allocations $\boldsymbol{p_o, p_u}$, and the detection threshold ε_i^j of each SU that maximize the average energy efficiency of the secondary users in the hybrid multi-clustered RF-CRN. The optimization problem to determine the optimal sensing parameters and power allocations in the hybrid multi-channel access based RF-CRN can hence be formulated as follows in P1.

Problem P1

$$\max_{\tau_s, \{\varepsilon\}, \{p_o\}, \{p_u\}} \frac{R(\tau_s, \boldsymbol{\varepsilon}, \boldsymbol{p_o}, \boldsymbol{p_u})}{E_c(\tau_s, \boldsymbol{\varepsilon}, \boldsymbol{p_o}, \boldsymbol{p_u})} \qquad (22)$$

$$subject \; to: I_s^j \leq I_{max} \qquad (C1)$$
$$E_{i,n} - E_{c,i} \geq 0 \qquad (C2)$$
$$0 \leq \tau_s \leq (T - \tau_r) \qquad (C3)$$
$$p_{av,i} \leq p_{max} \qquad (C4)$$
$$p_o \geq 0, \quad p_u \geq 0 \qquad (C5)$$
$$\forall \, i \in \{1, \cdots, n_t\}$$

The expression in (22) defines the objective function, (C1) guarantee the protection of PU against interference from SUs, while (C2) and (C3) ensure that the energy causality and time causality constraints are satisfied. P1 defines a more complex problem than those in the literature. The problem takes into consideration the effect of both the inter-cluster and intra-cluster interference on the PU transmission as shown in constraint (C1). P1 equally expresses a practical scenario where, the achievable capacity of the SUs transmission as expressed in (18) is not only limited by Additive White Gaussian Noise (AWGN) and the intra-cluster interference from PU transmission in the respective cluster as commonly assumed in e.g., [17], [22], [23].

The problem in P1 is a fractional nonlinear problem where, the maximum energy efficiency q^* of the considered system can be defined as

$$q^* = \frac{R(\tau_s, \boldsymbol{\varepsilon}, \boldsymbol{p_o}, \boldsymbol{p_u})}{E_c(\tau_s, \boldsymbol{\varepsilon}, \boldsymbol{p_o}, \boldsymbol{p_u})}$$
$$= \max_{\tau_s, \boldsymbol{\varepsilon}, \boldsymbol{p_o}, \boldsymbol{p_u}} \frac{R(\tau_s, \boldsymbol{\varepsilon}, \boldsymbol{p_o}, \boldsymbol{p_u})}{E_c(\tau_s, \boldsymbol{\varepsilon}, \boldsymbol{p_o}, \boldsymbol{p_u})} \qquad (23)$$

The fractional objective function in (23) is equivalent to a subtractive form expressed as $f(x) = R(x) - qE_c(x)$ [26]. Therefore, the energy efficiency q^* is maximized *if and only if*

$$\max_{\tau_s, \boldsymbol{\varepsilon}, \boldsymbol{p_o}, \boldsymbol{p_u}} R(\tau_s, \boldsymbol{\varepsilon}, \boldsymbol{p_o}, \boldsymbol{p_u}) - qE_c(\tau_s, \boldsymbol{\varepsilon}, \boldsymbol{p_o}, \boldsymbol{p_u})$$
$$= R(\tau_s, \boldsymbol{\varepsilon}, \boldsymbol{p_o}, \boldsymbol{p_u}) - q^* E_c(\tau_s, \boldsymbol{\varepsilon}, \boldsymbol{p_o}, \boldsymbol{p_u}) = 0 \qquad (24)$$

for $R(\tau_s, \boldsymbol{\varepsilon}, \boldsymbol{p_o}, \boldsymbol{p_u}) \geq 0$ and $E_c(\tau_s, \boldsymbol{\varepsilon}, \boldsymbol{p_o}, \boldsymbol{p_u}) > 0$.

Therefore, the original problem in **P1** can now be written as

Problem P2

$$\max_{\tau_s, \boldsymbol{\varepsilon}, \boldsymbol{p_o}, \boldsymbol{p_u}} R(\tau_s, \boldsymbol{\varepsilon}, \boldsymbol{p_o}, \boldsymbol{p_u}) - qE_c(\tau_s, \boldsymbol{\varepsilon}, \boldsymbol{p_o}, \boldsymbol{p_u})$$
$$Subject \; to: (C1), (C2), (C3), (C4), (C5) \qquad (25)$$

The problem in P2 expresses a non-linear optimization problem (NLP) that is non-convex jointly in τ_s, p_o and p_u. There is also a high degree of coupling among the optimization variables, which makes direct decomposition difficult.

III. RESOURCE ALLOCATION IN THE MULTI-CHANNEL ACCESS CRNs

The objective function in problem P2 is nonlinear and non-convex. In order to solve the problem we employ the method

of alternating convex optimization technique [27]. That is, for a fixed sensing time, we first obtain the transmit power allocation. Following this, the sensing duration is obtained, and vice-versa iteratively until the algorithm converges.

1) TRANSMISSION POWER ALLOCATION

Following the alternate convex optimization method of solution, the problem to determine the transmission power allocation in problem P2 can be written as follows

Problem P3

$$\max_{\boldsymbol{p_o}, \boldsymbol{p_u}} \{R(\tau_s, \boldsymbol{\varepsilon}, \boldsymbol{p_o}, \boldsymbol{p_u}) - qE_c(\tau_s, \boldsymbol{\varepsilon}, \boldsymbol{p_o}, \boldsymbol{p_u})\}|_{(\tau_s,)}$$

$$subject\, to : (C1), (C2), (C3), (C4)\text{ and }(C5) \qquad (26)$$

The optimization problem in P3 is nonlinear but convex w.r.t p_o and p_u. Using the Lagrangian multiplier approach, the Lagrangian $\mathcal{L}(\boldsymbol{p_o}, \boldsymbol{p_u}, \lambda, \boldsymbol{\beta}, \boldsymbol{\alpha})$ of problem P3 is given by

$$\mathcal{L}(\boldsymbol{p_o}, \boldsymbol{p_u}, \lambda, \boldsymbol{\beta}, \boldsymbol{\alpha})$$
$$= R(\tau_s, \boldsymbol{\varepsilon}, \boldsymbol{p_o}, \boldsymbol{p_u}) - qE_c(\tau_s, \boldsymbol{\varepsilon}, \boldsymbol{p_o}, \boldsymbol{p_u})$$
$$+ \sum_{i=1}^{n_t} \beta_i(I_{max} - I_s^j)$$
$$+ \sum_{i=1}^{n_t} \lambda_i \left(E_{i,n} - E_{c,i}\right)$$
$$+ \sum_{i=1}^{n_t} \alpha_i \left(p_{max} - p_{av,i}\right)$$

$$Subject\, to : p_o \geq 0, \quad p_u \geq 0 \qquad (27)$$

where $\lambda = \{\lambda_i\}$, $\boldsymbol{\beta} = \{\beta_i\}$, and $\boldsymbol{\alpha} = \{\alpha_i\}, \forall i = \{1, \cdots, n_t\}\}$ is the non-negative Lagrangian multiplier associated with the interweave and underlay power allocations for each secondary user, and

$$\boldsymbol{p_o} = \begin{pmatrix} p_{o,1} \\ p_{o,2} \\ \vdots \\ p_{o,n_t} \end{pmatrix}, \quad \boldsymbol{p_u} = \begin{pmatrix} p_{u,1} \\ p_{u,2} \\ \vdots \\ p_{u,n_t} \end{pmatrix}, \quad \boldsymbol{q} = \begin{pmatrix} q_1 \\ q_2 \\ \vdots \\ q_{n_t} \end{pmatrix}$$

The dual problem of (26) can be given by

$$\min_{\lambda, \boldsymbol{\beta}, \boldsymbol{\alpha} \geq 0} g(\lambda, \boldsymbol{\beta}, \boldsymbol{\alpha}) \qquad (28)$$

while, the Lagrangian dual function $g(\lambda, \boldsymbol{\beta}, \boldsymbol{\alpha})$ is represented by

$$g(\lambda, \boldsymbol{\beta}, \boldsymbol{\alpha}) = \max_{\boldsymbol{p_o}, \boldsymbol{p_u} \geq 0} \mathcal{L}(\boldsymbol{p_o}, \boldsymbol{p_u}, \lambda, \boldsymbol{\beta}, \boldsymbol{\alpha}) \qquad (29)$$

By taking the derivative of (27) with respect to (w.r.t) $\boldsymbol{p_o}$ and $\boldsymbol{p_u}$, and then set each equal to zero, the values of p_o and p_u that maximize $\mathcal{L}(\boldsymbol{p_o}, \boldsymbol{p_u}, \lambda, \boldsymbol{\beta}, \boldsymbol{\mu})$ can be determined from Karush-Kuhn-Tucker (KKT) conditions as in (30) and (31), shown at the bottom of the next page. The expressions in (30) and (31), provide us with insight to the effects of the SU transmitter to SU receiver channel gain $h_{i,r}$, interference channel gain from the PU transmitter to the SU receiver

h_r^j, from the SU transmitters to the PU receiver $h_i^{j,r}$, and the inter-cluster interference on the power allocation strategy. In particular, both transmit power, i.e., $p^{j'}_{o,i|(\sigma_{un}^{j'} \neq 0, \sigma_{ov}^{j'} \neq 0)}$ and $p^{j'}_{u,i|(\sigma_{un}^{j'} \neq 0, \sigma_{ov}^{j'} \neq 0)}$, increase when the direct channel for data transmission $h_{i,r}$ is good. The underlay transmit power reduces when the interference channels $h_i^{j'}$ is good. More importantly, the effect of the interference from SUs transmission in the other cluster is captured in (30) and (31) where, both transmit power reduce with increasing interference $\sigma_{i',(un)}^j$, and $\sigma_{i',(ov)}^{j'}$ from the SUs in cluster j'.

The Lagrangian dual variables are iteratively updated using a sub-gradient approach as follows, i.e.

$$\beta_i^{t+1} = \beta_i^t + \delta_{\boldsymbol{\beta}} \left(I_{max} - I_s\right) \qquad (32)$$

$$\lambda_i^{t+1} = \lambda_i^t + \delta_{\lambda} \left(E_{i,n} - E_{c,i}\right) \qquad (33)$$

$$\alpha_i^{t+1} = \alpha_i^t + \delta_{\boldsymbol{\alpha}} \left(p_{max} - p_{av,i}\right) \qquad (34)$$

until convergence towards a feasible optimal solution $\{\lambda^*, \boldsymbol{\beta}^*, \boldsymbol{\alpha}^*\}$. The parameters $\delta_{\lambda}, \delta_{\boldsymbol{\beta}}$, and $\delta_{\boldsymbol{\alpha}}$ denote step-sizes for the dual variables. It is important to note that the target is to determine the transmit powers of SU i i.e. $(p_{o,i}, p_{u,i})$, therefore to simplify analysis, it is assumed that $p_{o,i'}(t + 1) = \bar{p}_{o,i}(t)$, and $p_{u,i'}(t + 1) = \bar{p}_{u,i}(t)$ in (18), (30) and (31)

2) SENSING DURATION

In the objective function of problem P2, τ_s only appears in $((T - \tau_s - \tau_r)/T)$, but it is intertwined with τ_c by $\tau_s = K\tau_c$, such that $\tau_c = (\tau_s/K)$. Therefore, τ_c can be replaced by (τ_s/K) in subsequent expressions. We assume that a target Q_D is pre-defined and ε can be adjusted to satisfy this target. Hence, (1) is equivalent to (35)

$$\varepsilon_i^j = \sqrt{\frac{2\gamma_i^j + 1}{(\tau_s f_s/K)}} Q^{-1}(P_D^{th}) + \gamma_i^j + 1 \qquad (35)$$

where, the expected probability of detection for each SU P_D^{th} that satisfies the target Q_D^{th} based on OR-fusion rule could be obtained as

$$P_{D,j}^{th} = 1 - \exp\left(\frac{\log_e(1 - Q_D^{th})}{\sum_{i=1}^N x_{i,j}}\right), \qquad \forall j \in \{1, \ldots, M\},$$

The probability of false alarm in (2) can therefore be re-written as (36)

$$P_{F,i}^j = Q\left(\sqrt{(2\gamma_i^j + 1)}Q^{-1}\left(P_D^{th}\right) + \gamma_i^j \sqrt{(\tau_s f_s/K)}\right). \qquad (36)$$

Hence, problem P2 can be written in terms of τ_s such that, the sensing time can be obtained using a one-dimensional search algorithm from the objective function in P2, given $\boldsymbol{p_o}$, and $\boldsymbol{p_u}$. This method follows the method used in literature [23], [24]. Algorithm 1 gives the summary of the solution method in Section III.

The complexity of Algorithm 1 comprises of the complexity of the sub-gradient, the search method for the sensing

Algorithm 1 Joint Resource Allocation in Energy Harvesting Based Cognitive Radio Networks

1: **procedure** Resource Allocation in EH-CRN.
2: **Input** Q_D^{th}, χ
3: Initialize p_o, p_u, q, β, λ
4:     **for** $\tau_s = 0 : 0.017 * (T - \tau_r) : T - \tau_r$ **do**
5:         **for** $i = 1 : N$ **do**
6: **repeat**
7:     Set $q = (R(\tau_s, p_o, p_u)/E_c(\tau_s, p_o, p_u))$
8: **repeat**
9: **update** dual variables using sub-gradient method
10: **update** $p_{o,i}$, and $p_{u,i}$ from (30) and (31)
11: **until** $p_o^\delta == p_o^{\delta-1}$, $p_u^\delta == p_u^{\delta-1}$
12: **update** $E_{i,c}$, R_i, I_s and $p_{ave,i}$
13: **until** constraints are all satisfied
14: **return** $p_{(\tau_s)}^{o+} = p^{o+}$, $p_{(\tau_s)}^{u+} = p^{u+}$, $q_{(\tau_s)}^+ = q$
15:         **end for**
16: $\tau_s^* = \arg\max_{\tau_s} q_{(\tau_s)}^+$, $p_o^* = p_{o,(\tau_s^*)}$, $p_u^* = p_{u,(\tau_s^*)}$
17: Evaluate $\varepsilon_{i,j}^*$ from (42)
18:     **end for**
19: **Output**: $\{p_o^*\}$, $\{p_u^*\}$, τ_s^*, $\{\varepsilon^*\}$
20: **end procedure**

time, the time to execute the functions in line (10), and the number of iterations before convergence for every SU. The dual sub-gradient algorithm is known to achieve an ϵ-approximate solution with convergence time $\mathcal{O}\left(\frac{K_\epsilon}{\epsilon^2}\right)$ [28] where, K_ϵ represents the number of the constraints (dual variables) while, the the search method for the sensing time takes $\frac{T}{\Delta\tau_s}$. We assume it takes a constant time ϖ to executes each of the functions in line (10) to update p_o and p_u for every SU until convergence. Therefore, the total complexity

of the proposed algorithm is $\mathcal{O}\left((n_t)^3 \log n_t \frac{T}{\Delta\tau_s} \varpi \frac{K_\epsilon}{\epsilon^2}\right)$ (which comprise of the two nested while loops inside the two for loops). It is important to note that when the initial points and the step sizes of the dual variables are suitably chosen, the sub-gradient method and the algorithm can converge more quickly. On the other hand, the total complexity of the algorithm in [23] can be evaluated as $\mathcal{O}\left((n_t)^3 \log n_t \frac{T}{\Delta\tau_s} \varrho \frac{C_\epsilon}{\epsilon^2}\right)$ given n_t SUs where, ϱ $(< \varpi)$ and C_ϵ $(< K_\epsilon)$ denote the constant time it takes to execute (p_o, p_u) and, the number of the dual variables respectively.

$$
\begin{aligned}
&R(\tau_s, p_{o,i}, p_{u,i})\big|_{(\sigma_{un}^{j'}=0, \sigma_{ov}^{j'}=0)} \\
&= \frac{\tau_T}{n_t T}\Bigg[P_{H_0}\left(1 - Q_F^j\right) \sum_{i=1}^{n_t} \log_2\left(1 + \frac{h_{i,r} p_{o,i}^j}{N_0}\right) \\
&\quad + P_{H_1}\left(1 - Q_D^j\right) \sum_{i=1}^{n_t} \log_2\left(1 + \frac{h_{i,r} p_{o,i}^j}{N_0 + \sigma_{PU}^j}\right) \\
&\quad + P_{H_0} Q_F^j \sum_{i=1}^{n_t} \log_2\left(1 + \frac{h_{i,r} p_{u,i}^{j'}}{N_0}\right) \\
&\quad + P_{H_1} Q_D^j \sum_{i=1}^{n_t} \log_2\left(1 + \frac{h_{i,r} p_{u,i}^{j'}}{N_0}\right) \Bigg]
\end{aligned}
\tag{37}
$$

A. CASE FOR NO INTER-CLUSTER INTERFERENCE
For sufficiently large distance of separation between the two clusters, in particular between the receiver of cluster j and transmitters in j', the path loss can becomes considerably high resulting in the channel gain $h_{i',r}$ approaching zero. By setting $h_{i',r} = 0$ in (18), the inter-cluster interference from the PU and SUs in the j' cluster can be assumed equal to zero i.e., $\sigma_{i',(un)}^j = 0$, $\sigma_{i',(ov)}^{j'} = 0$, and $\sigma_{PU}^{j'} = 0$ in (19). Therefore, the

$$
p_{o,i}^j\big|_{\sigma_{un}^{j'}\neq0, \sigma_{ov}^{j'}\neq0} = \left\{ \frac{X_{1,2}^j}{2\log(2)K_{o1}} - \frac{\sigma_1 + v_0}{2h_{i,r}} \pm \sqrt{\left(\frac{X_{1,2}^j}{2\log(2)K_{o1}} - \frac{\sigma_1 + v_0}{2h_{i,r}}\right)^2 - \frac{\sigma_1 v_0}{h_{i,r}} + \frac{X_1^j v_0 + X_2^j(N_0 + \sigma_{PU}^j)}{\log(2)h_{i,r}K_{o1}}} \right\}^+
\tag{30}
$$

$$
p_{u,i}^{j'}\big|_{\sigma_{un}^{j'}\neq0, \sigma_{ov}^{j'}\neq0} = \frac{P_{H_1}Q_d^j + P_{H_0}Q_f^j}{\log(2)\left(P_{H_1}Q_d^j + P_{H_0}Q_f^j\right)[q_i + \lambda_i + \alpha_i] + \beta_i h_i^{j'}\left(P_{H_1}'(1 - Q_d^{j'}) + P_{H_0}'Q_d^{j'}\right)} - \frac{N_0 + \sigma_{PU}^{j'} + \sigma_{i',(ov)}^{j'}}{h_{ir}}
\tag{31}
$$

where,

$$
K_{o1} = X_{1,2}^j\left[q_i - \lambda_i\left(\eta \sum_{\substack{i=1,k=1 \\ i\neq k}}^{n_t} h_{i,k} - 1\right) + \alpha_i\right] + \beta_i h_i^j X_2^j,
$$

$$
\sigma_1 = N_0 + \sigma_{i',(un)}^j, \quad v_0 = \sigma_1 + \sigma_{PU}, \quad \sigma_{PU}^{j'} = p_p^{j'} h_r^{j'}, \quad \sigma_{PU}^j = p_p^j h_r^j
$$

$$
\sigma_{i',(un)}^j = \left(P_{H_1}'Q_D^{j'} + P_{H_0}'Q_F^{j'}\right) p_{u,i'} h_{i',r}, \quad \sigma_{i',(ov)}^{j'} = \left(P_{H_1}'(1 - Q_D^{j'}) + P_{H_0}'(1 - Q_F^{j'})\right) p_{o,i'} h_{i',r}
$$

$$
X_1^j = P_{H_1}(1 - Q_F^j), \quad X_2^j = P_{H_1}(1 - Q_D^j), \quad X_{1,2}^j = X_1^j + X_2^j
$$

and, $\{x\}^+ := \max\{0, x\}$.

expressions in (18) and (21) reduce to (37) and (38).

$$I_s \mid_{(\sigma_{un}^{j'}=0, \sigma_{ov}^{j'}=0)} = h_i^j p_{o,i} P_{H_1}(1 - Q_D^j) \tag{38}$$

respectively. Following the same analysis as in the preceding section, the expression for interweave and underlay power allocation can be written as in (39) and (40), as shown at the bottom of the page.

B. CASE FOR SINGLE CHANNEL ACCESS

In the case of conventional single transmission frequency (i.e. hybrid single-channel access) as existing in the literature, (18) and (21) reduce to (41) and (42) [17], [18], [19], [22], [23], [24])

$$\hat{R}(\tau_s, p_{o,i}, p_{u,i})$$

$$= \frac{\tau_T}{n_t T} \left[P_{H_0}\left(1 - Q_F^j\right) \sum_{i=1}^{n_t} log_2\left(1 + \frac{h_{i,r} p_{o,i}^j}{N_0}\right) \right.$$

$$+ P_{H_1}\left(1 - Q_D^j\right) \sum_{i=1}^{n_t} log_2\left(1 + \frac{h_{i,r} p_{o,i}^j}{N_0 + \sigma_{PU}^j}\right)$$

$$+ P_{H_0} Q_F^j \sum_{i=1}^{n_t} log_2\left(1 + \frac{h_{i,r} p_{u,i}^j}{N_0}\right)$$

$$\left. + P_{H_1} Q_D^j \sum_{i=1}^{n_t} log_2\left(1 + \frac{h_{i,r} p_{u,i}^j}{N_0 + \sigma_{PU}}\right) \right] \tag{41}$$

and

$$\hat{I}_s = h_i^j p_{o,i} P_{H_1}(1 - Q_D^j) + h_i^j p_{u,i} P_{H_1} Q_D^j \tag{42}$$

respectively. The interweave and underlay power allocation can subsequently be obtained as (43) and (44), shown at the bottom of the next page.

IV. SIMULATION RESULTS

This section presents the simulation results of the energy harvesting cognitive radio network. We assume two clusters j and j') separated about 400 meters from each other. In each cluster, there are $n_t = 10$ SUs transmitters in a $100m \times 100m$ square area, and an SU receiver located at the top right-hand corner of each cluster. At the center of each cluster a PU transmitter is deployed. The 2 PUs transmitters are therefore

Symbol	Description	Value
f_s	Sampling frequency	100 MHz
p_s	Sensing power	110 mW
p_r	Reporting power	410 mW
T	Frame duration	200 ms
n	Number of frames	2
τ_r	Reporting time	50 ms
$P(H_0)$	Probability that channel is not occupied by PU	0.7
$P(H_1)$	Probability that a channel is occupied by PU	0.3
N_0	Noise power	0 dBm
I_{max}	Maximum interference allowed on PU signal	-3 dBm
Q_D	Target probability of detection	0.9

about 700 meters from each other and their receivers are respectively located at the bottom edge corner of each cluster. Therefore, for SUs in cluster j, their PTC is denoted as f_j while $f_{j'}$ denotes their BTC. Likewise, for SUs in cluster j', channel $f_{j'}$ is their PTC while f_j their BTC. Hence channel f_j (cluster j) and channel $f_{j'}$ (cluster j') are twin channels (clusters). Our analysis is focused on evaluating the performance of the SUs in cluster j while, it is assumed that the interweave and underlay transmit powers of SUs in cluster j' i.e., $(p_{o,i'}^{j'}, p_{u,i'}^{j'})$ at time t is the average of the interweave and underlay transmit powers of SUs in cluster j i.e., $(p_{o,i}^j, p_{u,i}^{j'})$ at time $(t-1)$ respectively as earlier indicated. Apart from the above, shown in Table 3 are the summary of the parameter values used for the simulation. These parameters are as used in e.g., [23], [29]) among other literature.

Figs. 4 and 5 show plots of total throughput (spectral efficiency) against sensing duration, and average energy efficiency against sensing duration at optimal transmit power. The figures show that optimal sensing duration, depends on the PU transmit power. It increases with reducing PU transmit power in Fig. 4 but, increases with increasing PU transmit power in Fig. 5. The plot in Fig. 6 explicitly provides insight into sensing duration necessary to maximize achievable total throughput and the average energy efficiency for varying PU transmit power. In order to maximize the achievable throughput, SUs need to adequately sense the PU channel in order to minimize incorrect sensing decisions. Therefore, SU spends more time to sense the PU channel at low PU transmit power

$$p_{o,i}^j \mid_{\sigma_{un}^{j'}=\sigma_{ov}^{j'}=0} = \frac{X_{1,2}^j}{2\log(2)K_{o2}} - \frac{N_0 + w_o}{2h_{i,r}} \pm \sqrt{\left(\frac{X_{1,2}^j}{2\log(2)K_{o2}} - \frac{N_0 + w_o}{2h_{i,r}}\right)^2 - \frac{N_0 w_o}{h_{i,r}} + \frac{X_1^j w_o + X_2^j N_0}{\log(2)h_{i,r}K_{o2}}} \tag{39}$$

$$p_{u,i}^{j'} \mid_{\sigma_{un}^{j'}=\sigma_{ov}^{j'}=0} = \frac{1}{\log(2)(q_i + \alpha_i + \lambda_i)} - \frac{N_0}{h_{i,r}}$$

$$K_{o2} = (X_1 + X_2)\left[q_i - \lambda_i\left(\eta \sum_{\substack{i=1,k=1 \\ i \neq k}}^{n_t} h_{i,k} - 1\right) + \alpha_i\right] + \beta_i h_i^j X_2, \quad \sigma_{PU} = p_p h_r^j$$

$$w_o = N_0 + \sigma_{PU}^j, \quad X_1^j = P_{H_1}(1 - Q_F^j), \quad X_2^j = P_{H_1}(1 - Q_D^j), \quad X_{1,2}^j = X_1^j + X_2^j \tag{40}$$
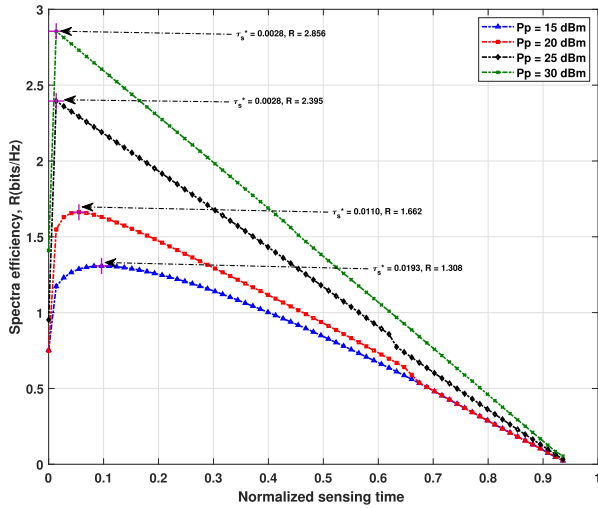
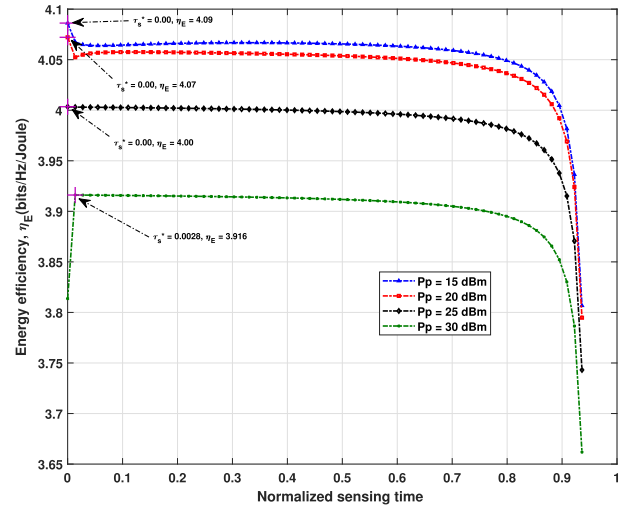**FIGURE 4.** Total achievable spectral efficiency against normalized sensing time at optimal p_o, p_u; ($p_{max} = 30$ *dBm*).

FIGURE 5. Average energy efficiency against normalized sensing time at optimal p_o, p_u; ($p_{max} = 30$ *dBm*).

but, the sensing duration reduces with increasing p_p. On the other hand, in order to maximize energy efficiency, the priority of SUs is to expend less energy (for sensing and data transmission) hence, the reduced sensing duration as shown. It is however, worth-noting that the effect of spectrum sensing is not as critical for energy efficiency maximization as it is for maximizing the throughput.

Fig. 7 shows average transmit power p_{ave} against p_{max} for different p_p. The plot shows that maximum p_{ave} exists for each SU (for a particular p_p), and it increases with increasing P_p. This is particularly so because as P_p increases, the amount of energy harvested increases, enabling SUs to adequately satisfy their energy expenditure. At the same time the amount of power the SU can transmit and the interference threshold allowed at the PU receiver, and the effect of imperfect sensing

constitute a bound on the maximum average power SUs can transmit. Hence, the SU maintains a constant average transmit power after reaching a certain peak value.

Figure 8 is a plot of average spectral efficiency against increasing p_{max} at different p_p. It shows that throughput increases with increasing p_p. This is expected since p_{ave} increases with p_p as shown in Fig. 7. The plot in Figure 8 also illustrates the behaviour of the spectral efficiency with increasing p_{max}. The reasons for this behaviour is that increasing p_{max} allows p_o and p_u to increase, and as the SU transmit power increases, the harvested energy increases with a corresponding increase in the average achievable throughput. Moreover, as the harvested energy increases, sensing accuracy also increases since the SU can adequately sense the channel thereby reducing the probability of false alarm. The

$$p_{o,i}|_{SF} = \frac{X_{1,2}^j}{2\log(2)K_{o,SF}} - \frac{N_0 + u_o}{2h_{i,r}} \pm \sqrt{\left(\frac{X_{1,2}^j}{2\log(2)K_{o,SF}} - \frac{N_0 + u_o}{2h_{i,r}}\right)^2 - \frac{N_0 u_o}{h_{i,r}} + \frac{X_1^j u_o + X_2^j N_0}{\log(2)h_{i,r}K_{o,SF}}} \quad (43)$$

$$p_{u,i}|_{SF} = \frac{X_{3,4}^j}{2\log(2)K_{u,SF}} - \frac{N_0 + u_o}{2h_{i,r}} \pm \sqrt{\left(\frac{X_{3,4}^j}{2\log(2)K_{u,SF}} - \frac{N_0 + u_o}{2h_{i,r}}\right)^2 - \frac{N_0 u_o}{h_{i,r}} + \frac{X_3^j u_o + X_4^j N_0}{\log(2)h_{i,r}K_{u,SF}}} \quad (44)$$

where,

$$K_{o,SF} = X_{1,2}^j \left[q_i - \lambda_i \left(\eta \sum_{\substack{i=1,k=1 \\ i \neq k}}^{n_t} h_{i,k} - 1 \right) + \alpha_i \right] + \beta_i h_i^j X_2^j,$$

$$K_{u,SF} = X_{3,4}^j [q_i + \lambda_i + \alpha_i] + \beta_i h_i^j X_4^j,$$

$$u_o = N_0 + \sigma_{PU}, \quad X_1^j = P_{H1}(1 - Q_F^j), \quad X_2^j = P_{H1}(1 - Q_D^j), \quad X_{1,2}^j = X_1^j + X_2^j$$

and,

$$X_3^j = P_{H0}Q_F^j, \quad X_4^j = P_{H1}Q_D^j,, \quad X_{3,4}^j = X_3^j + X_4^j$$
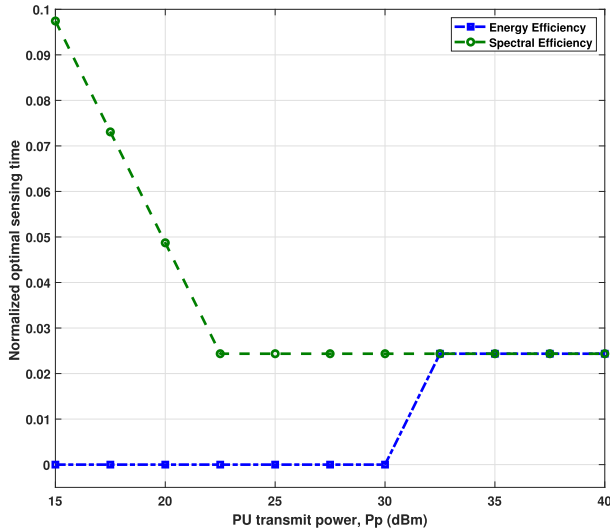
FIGURE 6. Optimal (normalized) sensing time that maximizes the total achievable throughput and the energy efficiency for varying PU transmit power at optimal p_o, p_u; ($p_{max} = 30\ dBm$).
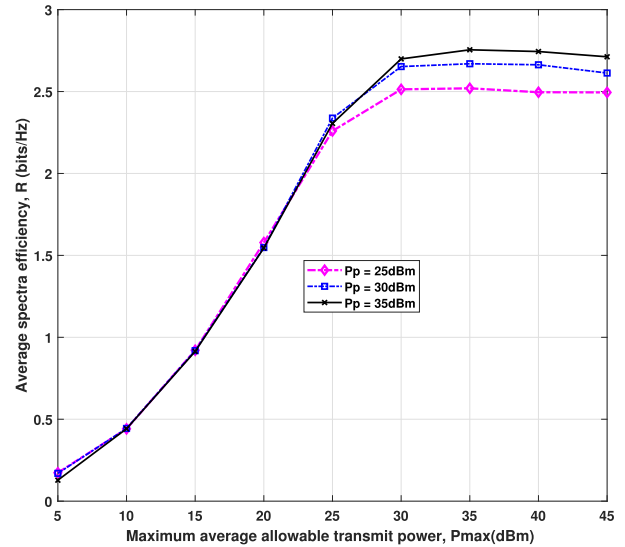

FIGURE 8. Total spectral efficiency against maximum allowed transmit power, p_{max} against ($\tau_s = 0.01$).
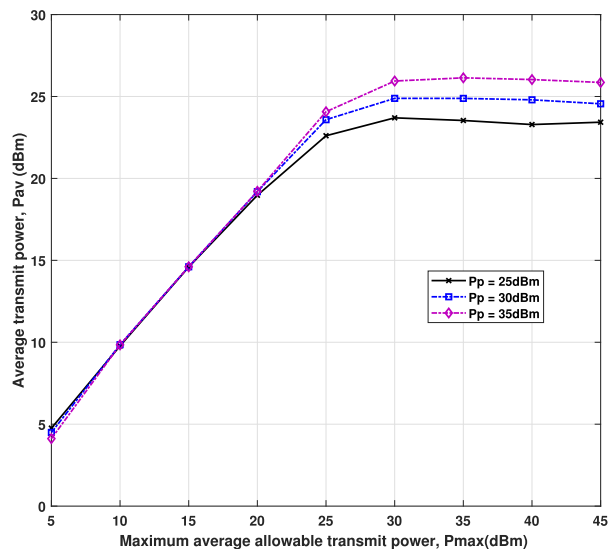

FIGURE 7. Average transmit power, p_{av} against maximum allowed transmit power, p_{max} against ($\tau_s = 0.01$).
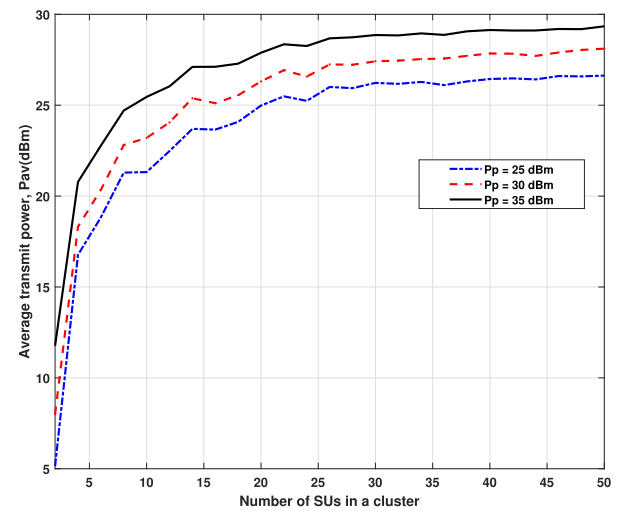

FIGURE 9. Average transmit power p_{av} against cluster size ($p_{max} = 30dBm$, $\tau_s = 0.01sec$).

lower the probability of false alarm, the more chances the interweave access whenever the channel is available [2], thus the higher the achievable throughput.

Figures 9, 10 and 11 illustrate the performance of the system with varying cluster size. Figure 9 shows that average transmit power increases with increasing number of users in the cluster. However, the rate of increase decreases as the cluster size increases. The increase in transmit power with increasing cluster size is the result of the increased harvesting period (as the number of SU increases, the transmit time for each SU reduces but, the proportion of the time available for energy harvesting increases), which translates to increased available energy and, consequently improved ability to transmit at the needed power.

The spectral efficiency as shown in Figure 10 increases with increasing in cluster size until a certain maximum is reached. At this point the sum throughput has reached the maximum and any addition to the number of users has no benefit but would only reduce the throughput of each SUs in the cluster. Therefore, the effect of the improved energy harvesting on the sum throughput is more prominent until an optimum cluster size reaches (about 30 SUs in this case). The possible conclusion here is that the performance of the network can be dwarfed due to insufficient energy budget but, the system can exploit the multi-user scenario by harvesting energy from other SUs, and the larger the cluster size the more energy that can be harvested. The only limitation however, is that as the cluster size increases the quantity of data that can be transmitted by each SU reduces. The energy efficiency as shown in Figure 11 is however independent of the cluster
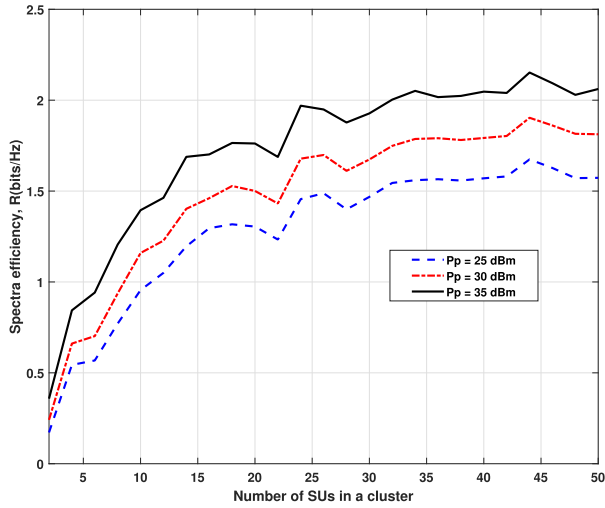
FIGURE 10. Spectra efficiency R against cluster size ($p_{max} = 30dBm$, $\tau_s = 0.01sec$).
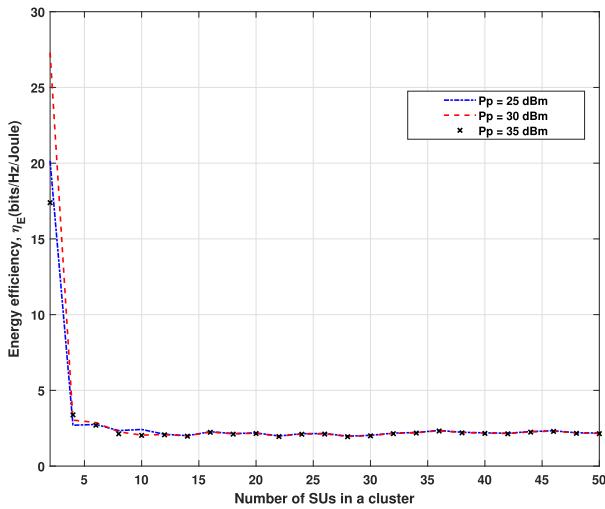

FIGURE 11. Energy efficiency η_E against cluster size ($p_{max} = 30dBm$, $\tau_s = 0.01sec$).

FIGURE 12. Average transmit power P_{ave} against maximum average transmit power p_{max} at optimal p_o, p_u and τ_s for different network models, $p_p = 43$ *dBm*.

FIGURE 13. Average energy efficiency η_E against maximum average transmit power p_{max} at optimal p_o, p_u and τ_s for different network models, $p_p = 43$ *dBm*.

size. In Figures 12, 13 and 14, we compared the performance of the following schemes

- Model 1 ($M1$): models a single-channel hybrid access as presented in [23]. Energy efficiency is defined as a ratio of the average achievable throughput to the net energy, i.e. $\eta_E = \frac{R(\tau_s,p_1,p_0)}{P_T+P_C-P_H}$, where, P_T, P_C and P_H are the average energy expended on data transmission, energy consumed in the SU transmitter circuit and, the harvested energy respectively. Performance of the EH-CRN is not energy constrained (N-EC).
- Model 2 ($M2$): models a single-channel hybrid access. Energy efficiency defined as the ratio of average achievable throughput to energy consumed. The performance of the EH-CRN is energy constrained (EC).
- Model 3 ($M3$): Proposed scheme

The plot in Figure 12 compares the average transmit power p_{ave} against p_{max} for various scenarios. It is necessary to state
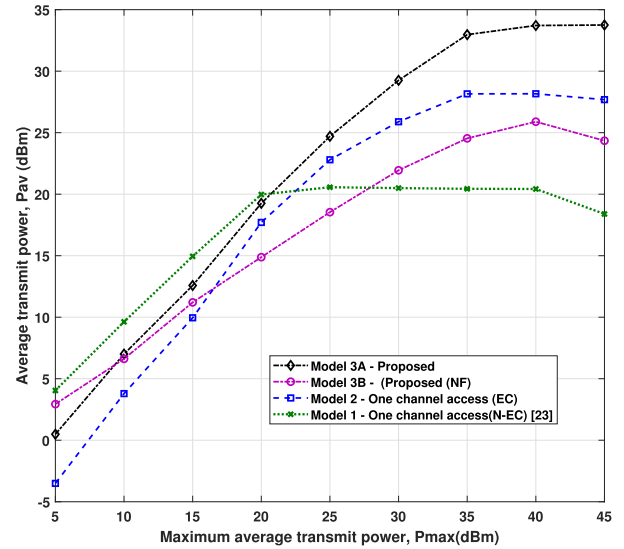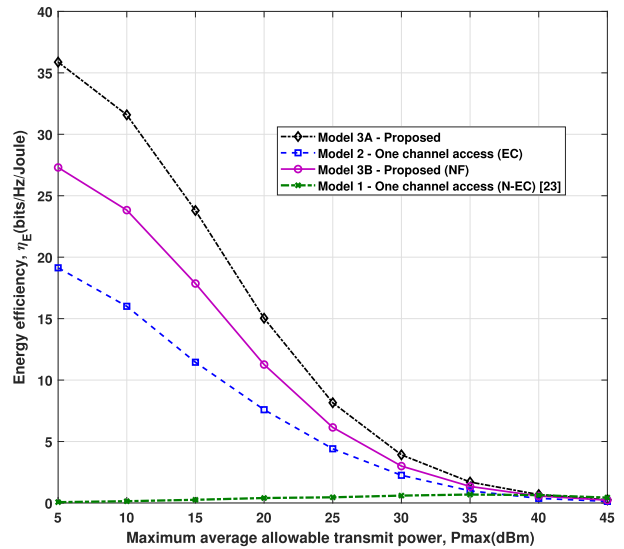
that while p_{ave} represents the average transmit power of the SU in $M1$ [23], $p_{ave} = (1/n_t) \sum_{i \in n_t} p_{ve,i}$ denotes the mean of the average transmit power in the multi-user cases of $M2$ and $M3$. In the figure, the results illustrate that SU transmit with higher average power in $M3$ (the proposed scheme) than the in $M2$. The technical explanation for this is that SU can transmit with relatively higher power on underlay mode with a reduced interference to the PU receiver due to increased distance between the SU transmitters and the PU receiver of the BTC in $M3$ than in $M2$. Results also show that SU in $M1$ [23] can transmit at higher p_{ave} than the schemes in $M2$ and $M3$ at lower p_{max} but, this is not unconnected to the fact that the performance of $M1$ in [23] is not energy
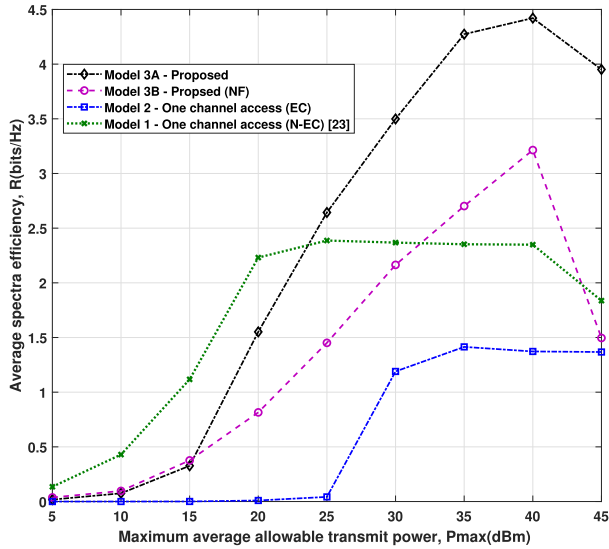
FIGURE 14. Total achievable spectra efficiency, R against maximum average transmit power p_{max} at optimal p_o, p_u and τ_s for different network models, $p_P = 43$ *dBm*.

constrained. However, at higher $p_{max}(\geq 20dBm)$ the proposed scheme outperforms the scheme in $M1$ because of the energy availability in $M3$ which increases with increasing p_{max}.

Figures 13 and 14 compare the performance of the proposed two-frequencies models in $M3A$ and $M3B$ with schemes $M1$ [23] and $M2$ in terms of spectral, and energy efficiency. Firstly, it is necessary to note that average energy efficiency is maximized at low SU transmit power. From Figures 13 and 14, the results for $M2$ and $M3$ show that achieving maximum energy efficiency and maximum spectral efficiency are conflicting objectives. Maximizing the spectral efficiency can only be achieved at high cost of energy expenditure because, the spectral efficiency can only be achieved with high transmit power. However, this results in high energy consumption and, consequently energy efficiency reduction. On the other hand, to obtain high energy efficiency, SUs need to transmit at the lowest possible power (translating to minimum spectral efficiency), in order to reduce energy budget.

More importantly, results in Figures 13 and 14 also show the relative performance of the proposed model when the two clusters are in close proximity (model 3B) and, when they are sufficiently far apart (model 3A). As the distance between the two clusters reduces, (resulting increasing inter-cluster interference), there is a performance degradation. The technical explanation to this behaviour is that as the distance between the two clusters increases, the inter-cluster interference from the SUs (transmitting underlay on the PTC), and the PU in cluster j' reduces while, the average underlay transmit power increases since there is reduction in $h_i^{j'}$ due to reduced path loss between the SU transmitter and the receiver of the PU in the j' cluster. The resultant effect of the probable increase in average underlay transmit power and, reduction in interference with increasing distance is the increased average spectral efficiency and average energy efficiency. On the other hand as the separation between the two clusters reduces, interference from SUs (transmitting underlay on the PTC) and the PU in cluster j' increases while the average underlay transmit power reduces to avoid degrading the QoS of the transmitting PU on the BTC. Therefore, the resultant effect of the probable decrease in the average underlay transmit power and, increase in interference with decreasing distance is reduced throughput and average energy efficiency. However, for $M1$ [23], there is no inter-cluster interference but the SU's average underlay transmit power could sufficiently be limited in order to avoid degrading the QoS of the nearby PU receiver. As a result the contribution from underlay transmission becomes negligible. The plot shows that the scheme in $M1$ has a better performance than the others at lower p_{max} but, that is not unconnected to the fact that it is not energy constrained. However, at p_{max} greater than about $24dBm$, the proposed scheme in $M3$ outperforms $M1$ because of the energy availability in $M3$ which, increases with increasing p_{max}. The presented results therefore show that our proposed scheme outperforms its counterpart single channel access scheme and equally performs better than the scheme in $M1$ at higher SU average transmit power. The benefit of the two-frequencies model, outweighs the effect of the inter-cluster interference which becomes negligible with increasing separation between the two clusters.

V. CONCLUSION
The work presented in this paper has investigated radio resource allocation and management in RF-CRNs towards maximizing energy efficiency in wireless devices. The investigation considered a practical multichannel, multi-user, overlapping cluster network where the heterogeneity of the SUs in terms of the SNR, and energy harvesting have been taken into consideration. The problem is formulated into a nonlinear optimization to determine the cooperative sensing parameters and, the optimal transmit power allocation suitable for the interweave-underlay hybrid access scheme in order to maximize the energy efficiency of SUs. The initial non-convex problem is transformed into a multiple convex problems, which is then solved using alternating convex optimization technique. Simulation results obtained show that there can be improved energy harvesting in the TDMA based RF-CRN for enhanced active probability and spectral efficiency of SUs if the multi-user scenario can be exploited such that SUs can harvest RF from other SU apart from the PU signal. Moreover, the larger the number of SUs sharing the harvesting channel (cluster size) the more energy that can be harvested and, consequently the better the spectral efficiency. However, as cluster size increases, the data rate of each SU decreases since, the time available for each SU to transmit decreases. A trade-off therefore, exists between harvested energy and the average achievable throughput of each SU, and an optimum number of SU exists where the average throughput of each SU is maximized. It is also worth-noting that optimizing spectral efficiency and energy efficiency are contradicting objectives.

A trade-off also exists between spectral efficiency and energy efficiency and therefore, the allocated SU transmit power depends on the primary design objective.

Moreover, results equally show that the proposed energy constrained two-frequencies model for the RF-CRN multi-channel access scheme where, each SU can opportunistically access two separate frequencies designated as PTC and BTC can provide considerable improvement in terms of spectral and energy efficiency over the one-frequency model.

REFERENCES

[1] A. Goldsmith, S. A. Jafar, I. Maric, and S. Srinivasa, "Breaking spectrum gridlock with cognitive radios: An information theoretic perspective," *Proc. IEEE*, vol. 97, no. 5, pp. 894–914, May 2009.

[2] Y.-C. Liang, Y. Zeng, E. C. Y. Peh, and A. T. Hoang, "Sensing-throughput tradeoff for cognitive radio networks," *IEEE Trans. Wireless Commun.*, vol. 7, no. 4, pp. 1326–1337, Apr. 2008.

[3] S. Yin, E. Zhang, J. Li, L. Yin, and S. Li, "Throughput optimization for self-powered wireless communications with variable energy harvesting rate," in *Proc. IEEE WCNC*, Apr. 2013, pp. 830–835.

[4] S. Yin, Z. Qu, and S. Li, "Achievable throughput optimization in energy harvesting cognitive radio systems," *IEEE J. Sel. Areas Commun.*, vol. 33, no. 3, pp. 407–422, Mar. 2015, doi: 10.1109/JSAC.2015.2391712.

[5] A. Celik, A. Alsharoa, and A. E. Kamal, "Hybrid energy harvesting-based cooperative spectrum sensing and access in heterogeneous cognitive radio networks," *IEEE Trans. Cogn. Commun. Netw.*, vol. 3, no. 1, pp. 37–48, Mar. 2017.

[6] A. Banerjee, S. P. Maity, and R. K. Das, "On throughput maximization in cooperative cognitive radio networks with eavesdropping," *IEEE Commun. Lett.*, vol. 23, no. 1, pp. 120–123, Jan. 2019.

[7] S. Biswas, S. Dey, and A. Shirazinia, "Sum throughput maximization in a cognitive multiple access channel with cooperative spectrum sensing and energy harvesting," *IEEE Trans. Cogn. Commun. Netw.*, vol. 5, no. 2, pp. 382–398, Jun. 2019.

[8] A. Alsharoa, N. M. Neihart, S. W. Kim, and A. El Kamal, "Multi-band RF energy and spectrum harvesting in cognitive radio networks," in *Proc. IEEE Int. Conf. Commun. (ICC)*, May 2018, pp. 1–6.

[9] M. Xu, M. Jin, Q. Guo, and Y. Li, "Multichannel selection for cognitive radio networks with RF energy harvesting," *IEEE Wireless Commun. Lett.*, vol. 7, no. 2, pp. 178–181, Apr. 2018.

[10] A. A. Olawole, F. Takawira, and O. O. Oyerinde, "Cooperative spectrum sensing in multichannel cognitive radio networks with energy harvesting," *IEEE Access*, vol. 7, pp. 84784–84802, 2019.

[11] X. Liu, K. Zheng, K. Chi, and Y.-H. Zhu, "Cooperative spectrum sensing optimization in energy-harvesting cognitive radio networks," *IEEE Trans. Wireless Commun.*, vol. 19, no. 11, pp. 7663–7676, Nov. 2020.

[12] S. Kusaladharma and C. Tellambura, "Aggregate interference analysis for underlay cognitive radio networks," *IEEE Wireless Commun. Lett.*, vol. 1, no. 6, pp. 641–644, Dec. 2012.

[13] T. M. C. Chu, H. Phan, and H.-J. Zepernick, "On the performance of underlay cognitive radio networks using M/G/1/K queueing model," *IEEE Commun. Lett.*, vol. 17, no. 5, pp. 876–879, May 2013.

[14] K. Pathak and A. Banerjee, "On energy cooperation in energy harvesting underlay cognitive radio network," in *Proc. 22nd Nat. Conf. Commun. (NCC)*, Guwahati, India, Mar. 2016, pp. 1–6.

[15] D. Xu and Q. Li, "Joint power control and time allocation for wireless powered underlay cognitive radio networks," *IEEE Wireless Commun. Lett.*, vol. 6, no. 3, pp. 294–297, Jun. 2017.

[16] K. Pathak, P. Bansal, and A. Banerjee, "Online time sharing policy in energy harvesting cognitive radio network with channel uncertainty," in *Proc. IEEE Global Commun. Conf. (GLOBECOM)*, Singapore, Dec. 2017, pp. 1–6, doi: 10.1109/GLOCOM.2017.8254598.

[17] K. Zheng, X. Liu, X. Liu, and Y. Zhu, "Hybrid overlay-underlay cognitive radio networks with energy harvesting," *IEEE Trans. Commun.*, vol. 34, no. 12, pp. 37–48, Jul. 2016.

[18] A. F. Tayel, S. I. Rabia, A. H. A. El-Malek, and A. M. Abdelrazek, "An optimal policy for hybrid channel access in cognitive radio networks with energy harvesting," *IEEE Trans. Veh. Technol.*, vol. 69, no. 10, pp. 11253–11265, Oct. 2020.

[19] A. F. Tayel, S. I. Rabia, A. H. A. El-Malek, and A. M. Abdelrazek, "Throughput maximization of hybrid access in multi-class cognitive radio networks with energy harvesting," *IEEE Trans. Commun.*, vol. 69, no. 5, pp. 2962–2974, May 2021.

[20] D. Xu and Q. Li, "Energy efficient joint channel and power allocation for energy harvesting cognitive radio networks," in *Proc. IEEE Int. Symp. Dyn. Spectr. Access Netw. (DySPAN)*, Oct. 2018, pp. 1–5.

[21] H. Xiao, H. Jiang, F. Shi, Y. Luo, L. Deng, M. Mukherjee, and M. J. Piran, "Energy-efficient resource allocation in radio-frequency-powered cognitive radio network for connected vehicles," *IEEE Trans. Intell. Transp. Syst.*, vol. 22, no. 8, pp. 5426–5436, Aug. 2021.

[22] G. Ozcan, M. C. Gursoy, N. Tran, and J. Tang, "Energy-efficient power allocation in cognitive radio systems with imperfect spectrum sensing," *IEEE J. Sel. Areas Commun.*, vol. 34, no. 12, pp. 3466–3481, Dec. 2016.

[23] K. Lee, C. Yoon, O. Jo, and W. Lee, "Joint optimization of spectrum sensing and transmit power in energy harvesting-based cognitive radio networks," *IEEE Access*, vol. 6, pp. 30653–30662, 2018.

[24] H. Xiao, H. Jiang, L.-P. Deng, Y. Luo, and Q.-Y. Zhang, "Outage energy efficiency maximization for UAV-assisted energy harvesting cognitive radio networks," *IEEE Sensors J.*, vol. 22, no. 7, pp. 7094–7105, Apr. 2022.

[25] Y. Wang, Y. Wang, F. Zhou, Y. Wu, and H. Zhou, "Resource allocation in wireless powered cognitive radio networks based on a practical non-linear energy harvesting model," *IEEE Access*, vol. 5, pp. 17618–17626, 2017.

[26] W. Dinkelbach, "On nonlinear fractional programming," *Manage. Sci.*, vol. 13, no. 7, pp. 492–498, Mar. 1967.

[27] A. Beck, "On the convergence of alternating minimization with applications to iteratively reweighted least squares and decomposition schemes," *SIAM J. Optim.*, vol. 25, no. 1, pp. 185–209, 2015.

[28] M. J. Neely and H. Yu, "Lagrangian methods for $\mathcal{O}(1/t)$ convergence in constrained convex programs," in *Convex Optimization: Theory, Methods, and Applications*, A. Ruud, Ed. Hauppauge, NY, USA: Nova Publishers, Jan. 2019.

[29] W. Saad, Z. Han, T. Basar, M. Debbah, and A. Hjørungnes, "Coalition formation games for collaborative spectrum sensing," *IEEE Trans. Veh. Technol.*, vol. 60, no. 1, pp. 276–297, Jan. 2011.

AKINBODE A. OLAWOLE received the Ph.D. degree from the University of the Witwatersrand Johannesburg, South Africa, in 2019. He is currently a Visiting Research Fellow with the School of Electrical and Information Engineering, University of the Witwatersrand, since 2020. His research interests include wireless communication systems and networks. He is a member of Academic Staff with Obafemi Awolowo University, Ile-Ife, Nigeria.

FAMBIRAI TAKAWIRA (Member, IEEE) received the Ph.D. degree from Cambridge University, U.K., in 1986. From 2012 to 2016, he was the Head of the School of Electrical and Information Engineering, University of the Witwatersrand Johannesburg, South Africa, where he is currently a Professor. Prior to that, he was a Professor and the Dean of the Faculty of Engineering, University of KwaZulu-Natal, Durban, South Africa. His research interests include wireless communication systems and networks. He has been an Active Volunteer of the IEEE ComSoc, the Director of Europe Middle East and Africa Region, from 2012 to 2013, a member of ComSoc Board of Governors, from 2012 to 2013, a member of ComSoc Nominations and Elections Committee, from 2012 to 2017, a member of COMSOC GIMS Committee, from 2013 to 2017, and a ComSoc Treasurer, from 2018 to 2021. He has also served as the General Co-Chair for the IEEE-AFRICON 2015, the Executive Co-Chair for International Conference on Communications 2010 (ICC2010), Cape Town, South Africa, and a member of Technical Committee at several IEEE AFRICON conferences. He was an Editor of the IEEE Transactions on Wireless Communications, from 2008 to 2010.

● ● ●